Onat, A. (2024). Application of a Modified Joint Unscented Kalman Filter for Parameter Estimation of a Class of Mechanical Systems. *The Black Sea Journal of Sciences*, 14(4), 2338-2357.

The Black Sea Journal of Sciences, 14(4), 2338-2357, 2024. DOI: 10.31466/kfbd.1561543

KFBD

Karadeniz Fen Bilimleri Dergisi
The Black Sea Journal of Sciences
ISSN (Online): 2564-7377 https://dergipark.org.tr/tr/pub/kfbd

Araştırma Makalesi / Research Article

Application of a Modified Joint Unscented Kalman Filter for Parameter Estimation of a Class of Mechanical Systems

Altan ONAT[1*]

Abstract

The unscented Kalman filter (UKF) is a tool for state and parameter estimation in nonlinear dynamical systems. There are two primary approaches for utilizing UKF in parameter and state estimation. The first approach is known as joint filtering, where both states and parameters are estimated concurrently. The second approach, dual filtering, involves the use of two separate filters to estimate states and parameters independently. Recently, a modified joint Unscented Kalman Filter (MJUKF) has been introduced by the author. This modified approach is applicable to a class of nonlinear systems and offers two significant advantages which are improved estimation accuracy and reduced computational complexity. This study investigates the application of the MJUKF for parameter estimation in two selected mechanical systems. The results demonstrate that the modified filter effectively estimates parameters in mechanical systems revealing its advantages over the standard joint unscented Kalman filtering method in terms of both accuracy and computational complexity.

Keywords: Unscented Kalman filter, Parameter estimation, Joint unscented Kalman filter, Coupled tank, Single link flexible joint.

Değiştirilmiş Kokusuz Kalman Filtresinin Parametre Tahmini için Bir Mekanik Sistem Sınıfına Uygulanışı

Öz

Kokusuz Kalman filtresi (KKF), doğrusal olmayan dinamik sistemlerde durum ve parametre tahmini için kullanılan bir araçtır. KKF'nin durum ve parametre tahmininde kullanılmasında iki ana yaklaşım bulunmaktadır. İlk yaklaşım hem durumların hem de parametrelerin eşzamanlı olarak tahmin edildiği birleşik filtreleme olarak bilinir. İkinci yaklaşım ise durum ve parametrelerin bağımsız olarak tahmin edildiği iki ayrı filtrenin kullanıldığı ikili filtreleme yöntemidir. Yakın zamanda, yazar tarafından Değiştirilmiş Birleşik Kokusuz Kalman Filtresi (DBKKF) tanıtılmıştır. Bu değiştirilmiş yaklaşım, doğrusal olmayan sistemlerin bir sınıfına uygulanabilir ve iki önemli avantaj sunar: iyileştirilmiş tahmin doğruluğu ve azaltılmış hesaplama karmaşıklığı. Bu çalışma, DBKKF'nin iki seçilmiş mekanik sistemde parametre tahmini için uygulanmasını incelemektedir. Sonuçlar, değiştirilmiş filtrenin mekanik sistemlerde parametreleri etkin bir şekilde tahmin ettiğini ve hem doğruluk hem de hesaplama karmaşıklığı açısından standart birleşik kokusuz Kalman filtreleme yöntemine göre avantajlarını ortaya koymaktadır.

Anahtar Kelimeler: Kokusuz Kalman Filtresi, Parametre tahmini, Birleşik kokusuz Kalman filtresi, Bağlı Tank, Tek bağlantılı esnek eklem.

[1]Eskisehir Technical University, Electrical and Electronics Engineering Department, Engineering Faculty, Eskisehir, Turkey, altanonat@eskisehir.edu.tr

[*]Sorumlu Yazar/Corresponding Author

Geliş/Received: 04.10.2024 **Kabul/Accepted:** 29.11.2024 **Yayın/Published:** 15.12.2024

1. Introduction

The Unscented Kalman Filter (UKF) is an alternative to the extended Kalman filter (EKF) that can be used for estimation in nonlinear dynamical systems. The UKF is a derivative-free filter for nonlinear estimation, and a Jacobian matrix is not necessary for the UKF as it is for the EKF. The core of the UKF is the unscented transformation through the points that are called sigma points. UKF can have a dual purpose, and it can be used both for state estimation and parameter estimation of nonlinear systems. There are two different approaches for parameter estimation. The first approach, known as joint filtering, employs a single filter to estimate a combined state vector that includes both states and parameters. The second approach involves the use of two separate filters, running simultaneously, for state and parameter estimation. In this approach, the output of the parameter estimator feeds into the input of the state filter (Van Der Merwe, 2004). A detailed discussion about the application of both approaches for parameter estimation is given in (Onat, 2019).

Both joint and dual types of Unscented Kalman Filters (UKF) are currently considered for state and parameter estimation in the literature. These filters are used in a variety of applications, including both electrical and mechanical systems. For example, the joint approach of UKF has been utilized to estimate the parameters of synchronous generators and regulators (González-Cagigal, Rosendo-Macías, & Gómez-Expósito, 2019). A similar methodology based on the joint Unscented Kalman Filter (JUKF) is applied to detect parameters in photovoltaic modules, along with system states and the hot-spot thermal model of power transformers by (González-Cagigal, Rosendo-Macías, & Gómez-Expósito, 2022) and (Gonzólez-Cagigal, Rosendo-Macías, & Gómez-Expósito, 2022), respectively. Another noteworthy application is the estimation of respiratory rate using JUKF for individuals based on wireless signals (Uysal, Onat, & Filik, 2020). These studies serve as examples of JUKF's implementation in electrical systems. Furthermore, JUKF based parameter estimation also extends to mechanical systems, with recent applications. For example, (Onat, Voltr, & Lata, 2018) presents the use of JUKF for estimating the rolling radius of traction wheels of low-floor trams. Additionally, (Onat & Kayaalp, 2020) reports the implementation of JUKF for estimating the normal load exerted on a traction wheel of a railway vehicle based on velocity measurements. JUKF has demonstrated its potential as a promising parameter estimator for mechanical systems. Dual filters can also be used as parameter estimators for electrical and mechanical systems. The states and parameters of a multi-axle heavy vehicle are estimated based on the dual filtering approach (Pei, Chen, Yang, & Chu, 2020). The state of charge (SoC) and parameters of a battery are detected by an improved adaptive dual unscented Kalman filter scheme (Peng, Zhang, Guo, & Zhang, 2021). However, since the cross-covariance matrix between states and parameters is not estimated in the

dual filtering framework, the accuracy of the parameter estimation results can be worse compared to the joint case. This fact is discussed in detail by (Van Der Merwe, 2004) and (Onat, 2019).

When UKF is used as a parameter estimator based on a joint structure, the number of sigma points that must be created depends on the number of states and parameters. JUKF creates $2L + 1$ sigma points where L is the length of the concatenated state vector. For example, if there are four states and two parameters, the concatenated state vector has six elements, and the number of sigma points must be thirteen for the standard JUKF. The proposed modified joint unscented Kalman filter (MJUKF) decouples parameters from the state vector, however, sigma points are using the values of parameter vector. MJUKF requires nine sigma points for the given example. The reduction of sigma points provides a decrease in computational complexity. This is the first advantage of the proposed approach. Secondly, MJUKF can be applied to nonlinear systems in which there is a linear relationship between measurements and parameters, and it creates a linear transformation between measurements and parameters; thus, the accuracy of the estimation can be improved based on the selection of filter parameters. Details of this modified scheme can be found in (Onat, 2019).

In this study, the application of this modified approach has been investigated and discussed for two selected mechanical systems. These systems are chosen since the MJUKF approach is applicable to systems with a linear relationship between the estimated parameters and the measurements. First, the structure of each selected mechanical system is presented. Then, the MJUKF approach is explained. Finally, the results demonstrating the advantages of the proposed approach are provided.

2. Models and the Proposed Method

2.1. Model of the Coupled Tank System

As the first application, the coupled tank system (Seung, Atiya, Parlos, & Chong, 2017) is selected in this study. Coupled tanks include two water tanks connected to each other by an orifice. There is also another orifice at the lower tank. There is a water basin and a water pump which pumps water to the upper tank from the basin. Water flows to the second tank from the orifice of the upper tank. Pump controls the water flow into the tanks, and this flow ratio is the input to the system. A schematic of the system can be found in Figure 1.

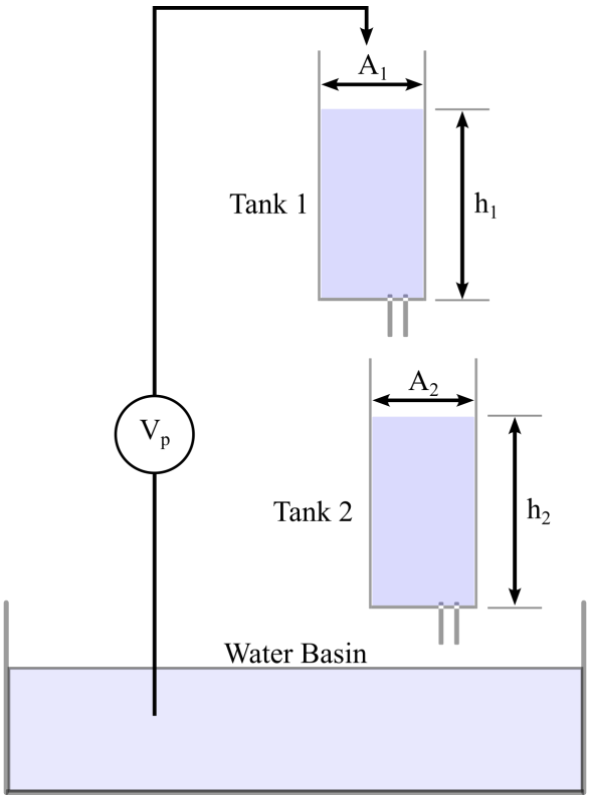

Figure 1 Schematic of the coupled tank system, adapted from (Seung, Atiya, Parlos, & Chong, 2017)

In this system, h_1 and h_2 are the water levels of the tanks. The mathematical equations of the system can be found in Equation (1) and Equation (2). System parameters that are considered can be found in Table 1.

$$\begin{aligned} \dot{h}_1 &= \frac{k_{flow} q_i - c_1 {h_1}^{1/2}}{A_1} \\ \dot{h}_2 &= \frac{c_1 {h_1}^{1/2} - c_2 {h_2}^{1/2}}{A_2} \end{aligned} \tag{1}$$

$$\begin{aligned} \dot{x} = \begin{bmatrix} \dot{h}_1 \\ \dot{h}_2 \end{bmatrix} &= \begin{bmatrix} \frac{-c_1 {h_1}^{1/2} + k_{flow} q_i}{A_1} \\ \frac{c_1 {h_1}^{1/2} + c_2 {h_2}^{1/2}}{A_2} \end{bmatrix} \\ \dot{x} = \begin{bmatrix} \dot{x}_1 \\ \dot{x}_2 \end{bmatrix} &= \begin{bmatrix} \frac{-c_1 {x_1}^{1/2} + k_{flow} u}{A_1} \\ \frac{c_1 {x_1}^{1/2} + c_2 {x_2}^{1/2}}{A_2} \end{bmatrix} \\ &= \begin{bmatrix} \frac{-c_1}{A_1} x_1^{1/2} \\ \frac{c_1}{A_2} x_1^{1/2} + \frac{c_2}{A_2} x_2^{1/2} \end{bmatrix} + \begin{bmatrix} \frac{k_{flow}}{A_1} \\ 0 \end{bmatrix} u \end{aligned} \tag{2}$$

Table 1 System parameters for coupled tank system, (Seung, Atiya, Parlos, & Chong, 2017)

System Parameters (Units)	Value
Cross-Sectional Areas of Tank 1, A_1 (cm^2)	15.5179
Cross-Sectional Areas of Tank 2, A_2 (cm^2)	15.5179
Orifice Coefficient of Tank 1, c_1	5
Orifice Coefficient of Tank 2, c_2	5
Pump Rate, q_i (Volts)	5
Flow Constant, k_{flow} ((cm^2/sec)/Volts)	6

2.2. Single-Link Flexible Joint Robot Model

It has been noted that the performance of most robots decreases when joint flexibility is not taken into account (Raghavan & Hedrick, 1994). This study considers the model of such a structure for estimation purposes. The relevant state-space equations for the system can be found in Equation (3) and Equation (4). In this equation, J_m is the inertia of the actuator (DC motor), J_l is the inertia of the controlled link. θ_m, ω_m, θ_l, ω_l are the angles and angular velocities of the motor and link, respectively. Angular velocities of the motor and link can differ when the torsional flexibility of the link is considered. B stands for the viscous friction in the motor bearing and back electromotive force effects. Other parameters in Equations below are given in Table 2, and an illustration of the system considered is given in Figure 2.

$$\begin{aligned}
\dot{\theta}_m &= \omega_m \\
\dot{\omega}_m &= \frac{k}{J_m}(\theta_l - \theta_m) - \frac{B}{J_m}\omega_m + \frac{K_\tau}{J_m}u \\
\dot{\theta}_l &= \omega_l \\
\dot{\omega}_l &= -\frac{k}{J_l}(\theta_l - \theta_m) - \frac{mgh}{J_l}sin(\theta_l)
\end{aligned} \tag{3}$$

$$\begin{aligned}
\dot{x} &= \begin{bmatrix} \dot{x}_1 \\ \dot{x}_2 \\ \dot{x}_3 \\ x_4 \end{bmatrix} = \begin{bmatrix} x_2 \\ \frac{k}{J_m}(x_3 - x_1) - \frac{B}{J_m}x_2 + \frac{K_\tau}{J_m}u \\ x_4 \\ -\frac{k}{J_l}(x_3 - x_1) - \frac{mgh}{J_l}\sin(x_3) \end{bmatrix} \\
&= \begin{bmatrix} x_2 \\ \frac{k}{J_m}(x_3 - x_1) - \frac{B}{J_m}x_2 \\ x_4 \\ -\frac{k}{J_l}(x_3 - x_1) - \frac{mgh}{J_l}\sin(x_3) \end{bmatrix} + \begin{bmatrix} 0 \\ \frac{K_\tau}{J_m} \\ 0 \\ 0 \end{bmatrix} u.
\end{aligned} \tag{4}$$

Table 2 System Parameters for a single-link robot with joint flexibility, *(Raghavan & Hedrick, 1994)* (Only K_τ is different)

System Parameters (Units)	Value
Motor Inertia, J_m (kg m^2)	3.7×10^{-3}
Link Inertia, J_l (kg m^2)	9.3×10^{-3}
Pointer mass, m (kg)	2.1×10^{-1}
Link Length, $2b$ (m)	3.0×10^{-1}
Torsional Spring Coefficient, k (Nm rad^{-1})	1.8×10^{-1}
Viscous Friction Coefficient, B (Nm V^{-1})	4.6×10^{-2}
Amplifier Gain, K_τ (Nm V^{-1})	15×10^{-2}

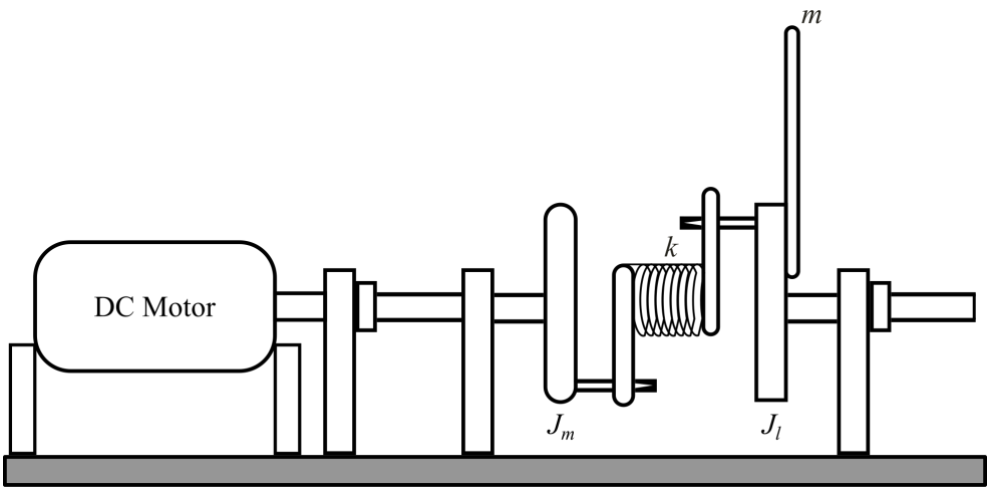

Figure 2 Representation of single-link robot with joint flexibility, adapted from (Raghavan & Hedrick, 1994)

It has been stated that the MJUKF can be considered when the measurements are linear with respect to the parameters. To show that the measurements can be written linearly in terms of the parameters, the system equations (Equation (3) and (4)) can be rewritten in the form of $\dot{x} = A\delta + B$,where δ includes the estimated parameters m and K_τ. This form can be expressed as:

$$\dot{x} = \begin{bmatrix} \dot{x}_1 \\ \dot{x}_2 \\ \dot{x}_3 \\ x_4 \end{bmatrix} = \begin{bmatrix} \dot{\theta}_m \\ \dot{\omega}_m \\ \dot{\theta}_l \\ \dot{\omega}_l \end{bmatrix} = \begin{bmatrix} 0 & 0 \\ 0 & \frac{u}{J_m} \\ 0 & 0 \\ -\frac{gh}{J_l}\sin(\theta_l) & 0 \end{bmatrix} \begin{bmatrix} m \\ K_\tau \end{bmatrix} + \begin{bmatrix} \omega_m \\ \frac{k}{J_m}(\theta_l - \theta_m) - \frac{B}{J_m}\omega_m \\ \omega_l \\ -\frac{k}{J_l}(\theta_l - \theta_m) \end{bmatrix} \quad (5)$$

A similar form can also be written for the coupled tank system. It should be noted that the estimated parameter is k_{flow}. There are four measurements and two parameters in the case of the single-link flexible joint robot model; therefore, the A matrix has dimensions 4x2. Similarly, for the coupled tank system, it must have dimensions 2x1.

2.2. Joint Unscented Kalman Filter and the Modified Filter

JUKF is a tool to estimate states and parameters of a nonlinear dynamical system, and this dynamical system in discrete (or discretized) form can be represented as:

$$\begin{aligned} \mathbf{x}_k &= f(\mathbf{x}_{k-1}, \mathbf{u}_{k-1}, \boldsymbol{\theta}_{k-1}) + \mathbf{q}_k \\ \mathbf{y}_k &= g(\mathbf{x}_k, \boldsymbol{\theta}_k) + \mathbf{r}_k, \end{aligned} \tag{6}$$

where $\mathbf{x}_k = \mathbf{x}(kT_s)$ is the discretized state vector with a discrete time index k and the sampling period T_s, $\mathbf{u}_k$ is the input vector, $\boldsymbol{\theta}$ is the parameter vector; model and measurement noise vectors are represented by $\mathbf{q}$ and $\mathbf{r}$, respectively. f and g are the nonlinear functions for system states and measurements, respectively as stated in (Onat, 2019).

The details of the standard JUKF as a parameter estimator is given in (Onat, 2019), and application of this standard JUKF to a mechanical system is presented in (Onat & Kayaalp, 2020). In addition, the algorithm for the JUKF can be found in Algorithm 1.

Algorithm 1. Joint Unscented Kalman Filter – Additive Noise Case (Onat & Kayaalp, 2020)

Define Filter Parameters
$L \leftarrow 3$ ▷ L is the dimension of state vector
$\alpha \leftarrow 1$ ▷ $(10^{-4} \leq \alpha \leq 1)$
$\kappa \leftarrow 0$ ▷ (generally $\kappa = 3 - L$)
$\beta \leftarrow 2$
$\lambda \leftarrow \alpha^2(L + \kappa) - L$
$\gamma \leftarrow \sqrt{L + \lambda}$
$W_0^{(m)} \leftarrow \dfrac{\lambda}{L + \lambda}$
$W_0^{(c)} \leftarrow \dfrac{\lambda}{L + \lambda} + 1 - \alpha^2 + \beta$
    for $i \leftarrow \{1, \cdots, 2L\}$ **do**
        $W_i^{(m)} \leftarrow W_i^{(c)} \coloneqq \dfrac{1}{2(L + \lambda)}$
    end for
End
function UKF$(\hat{\mathbf{x}}, \dot{\hat{\mathbf{x}}}, \mathbf{P})$
    Initialize
        $\hat{\mathbf{x}}_0 \leftarrow \mathrm{E}[\mathbf{x}_0]$
        $\mathbf{P}_0 \leftarrow \mathrm{E}[(\mathbf{x}_0 - \hat{\mathbf{x}}_0)(\mathbf{x}_0 - \hat{\mathbf{x}}_0)^T]$
    End
end function
function Sigma Points$(\hat{\mathbf{x}}, \mathbf{P})$
    Define
        $\mathbf{S}_{k\text{-}1} \leftarrow \sqrt{\mathbf{P}_{k\text{-}1}}$
    End
    for $k \in \{1, \cdots, \infty\}$ **do**
        $\boldsymbol{\chi}_{k-1} \leftarrow [\hat{\mathbf{x}}_{k-1}, \hat{\mathbf{x}}_{k-1} + \gamma\mathbf{S}_{k\text{-}1}, \hat{\mathbf{x}}_{k-1} - \gamma\mathbf{S}_{k\text{-}1}]$
    end for
end function

function Time Update($\boldsymbol{\chi}_{k-1}$, $\boldsymbol{P}$, $\mathbf{Q}$)

$\boldsymbol{\chi}^{*}_{k|k-1} \leftarrow \boldsymbol{f}(\boldsymbol{\chi}_{k-1}, u_{k-1})$

$\widehat{\boldsymbol{x}}^{-}_{k} \leftarrow \sum_{\boldsymbol{i=0}}^{\boldsymbol{2L}} \mathbf{W}_i^{(m)} \boldsymbol{\chi}^{*}_{i,k|k-1}$

$\mathbf{P}^{-}_{k} \leftarrow \sum_{\boldsymbol{i=0}}^{\boldsymbol{2L}} \mathbf{W}_i^{(c)} \left(\boldsymbol{\chi}^{*}_{i,k|k-1} - \hat{\mathbf{x}}^{-}_{k}\right)\left(\boldsymbol{\chi}^{*}_{i,k|k-1} - \hat{\mathbf{x}}^{-}_{k}\right)^{T} + \mathbf{Q}$

end function

function Measurement Update$\left(\boldsymbol{\chi}^{*}_{k|k-1}, \mathbf{R}\right)$

$\boldsymbol{\Upsilon}^{*}_{k|k-1} \leftarrow h\left(\boldsymbol{\chi}^{*}_{k|k-1}, \mathbf{u}_{k-1}\right)$

$\hat{\mathbf{y}}^{-}_{k} \leftarrow \sum_{\boldsymbol{i=0}}^{\boldsymbol{2L}} \mathbf{W}_i^{(m)} \boldsymbol{\Upsilon}^{*}_{i,k|k-1}$

$\mathbf{P}_{\tilde{\mathbf{y}}_k,\tilde{\mathbf{y}}_k} \leftarrow \sum_{\boldsymbol{i=0}}^{\boldsymbol{2L}} \mathbf{W}_i^{(c)} \left(\boldsymbol{\Upsilon}^{*}_{i,k|k-1} - \hat{\mathbf{y}}^{-}_{k}\right)\left(\boldsymbol{\Upsilon}^{*}_{i,k|k-1} - \hat{\mathbf{y}}^{-}_{k}\right)^{T} + \mathbf{R}$

$\mathbf{P}_{x_k,y_k} \leftarrow \sum_{\boldsymbol{i=0}}^{\boldsymbol{2L}} \mathbf{W}_i^{(c)} \left(\boldsymbol{\chi}^{*}_{i,k|k-1} - \hat{\mathbf{x}}^{-}_{k}\right)\left(\boldsymbol{\Upsilon}^{*}_{i,k|k-1} - \hat{\mathbf{y}}^{-}_{k}\right)^{T}$

$\mathbf{K}_k \leftarrow \mathbf{P}_{x_k,y_k}\mathbf{P}^{-1}_{\tilde{\mathbf{y}}_k,\tilde{\mathbf{y}}_k}$

$\hat{\mathbf{x}}_k \leftarrow \hat{\mathbf{x}}^{-}_{\boldsymbol{k}} + \mathbf{K}_k(\mathbf{y}_k - \hat{\mathbf{y}}^{-}_{k})$

$\mathbf{P}_k \leftarrow \mathbf{P}^{-}_{k} - \mathbf{K}_k\mathbf{P}_{\tilde{\mathbf{y}}_k,\tilde{\mathbf{y}}_k}\mathbf{K}^{T}$

end function

The main difference and novelty of the MJUKF is the incorporation of the parameter vector in the algorithm. Figure 3 illustrates this difference based on block diagrams. In JUKF, parameters are concatenated to the state vector, and estimation is done based on this vector. The MJUKF approach creates another sigma point vector for the parameter estimation. This vector can be given as

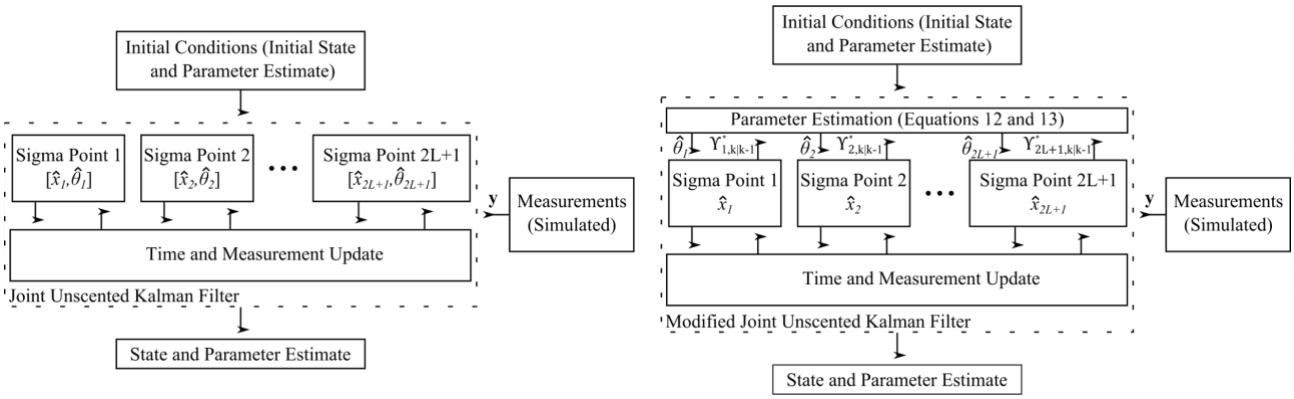

Figure 3 Comparison of JUKF and MJUKF based on block diagrams

$$\boldsymbol{\chi}_{\theta} = \begin{bmatrix} \widehat{\boldsymbol{\theta}}_1 \\ \widehat{\boldsymbol{\theta}}_2 \\ \vdots \\ \widehat{\boldsymbol{\theta}}_{\mathrm{n}} \end{bmatrix}, n = 2L + 1. \tag{7}$$

$\boldsymbol{\chi}_\theta$ represents the sigma point vector for parameters. L is the number of states in this case. Initial determination of the parameter vector can be written as

$$\widehat{\boldsymbol{\theta}}_i = \left(\widehat{\boldsymbol{\theta}}_0 - \mathbf{p}_\theta(L+1)\right) + \mathbf{p}_\theta i. \quad i = 1, \cdots, 2L+1 \tag{8}$$

i is the parameter vector index, $\mathbf{p}_\theta$ is a row vector containing initial parameter error covariance, $\widehat{\boldsymbol{\theta}}_0$ is the initial parameter estimate. After creating the parameter sigma points, the parameter sigma point is appended to the state sigma point matrix as $\boldsymbol{\chi}_{k-1}^{\dagger} = [\boldsymbol{\chi}_{k-1} | \boldsymbol{\chi}_\theta]$. Then, $\boldsymbol{\chi}_{k-1}^{\dagger}$ is propagated through the nonlinear function f of the system. The sigma point vector is also updated for the measurement sigma point as $\boldsymbol{\Upsilon}_{k|k-1}^{*} = g\left(\boldsymbol{\chi}_{k|k-1}^{*}\right)$. MJUKF updates the parameters in the parameter sigma point by considering the following rule:

$$\boldsymbol{\chi}_{\theta_{i,k}} = \widehat{\boldsymbol{\theta}}_{k-1} - \xi T\left(\mathbf{y}_k - \boldsymbol{\Upsilon}_{i,k|k-1}^{*}\right), i = 1, \ldots, 2L+1 \tag{9}$$

where ξ is a scaling parameter, T is a transformation matrix which transforms the error between the measurements $\mathbf{y}_k$ and the measurement sigma points $\boldsymbol{\Upsilon}_{i,k|k-1}^{*}$ at discrete time k. The selection of the parameters ξ and T is discussed in detail by (Onat, 2019). The last step of the MJUKF is the estimation of the parameter sigma point vector.

$$\widehat{\boldsymbol{\theta}}_k = \frac{1}{2L+1} \sum_{i=0}^{2L} \boldsymbol{\chi}_{\theta_i}. \tag{10}$$

Decoupling the parameters from sigma point vector in MJUKF results in less calculation of the nonlinear function f of the system. As an example, if there are four system states and two parameters, JUKF requires thirteen function evaluations, whereas MJUKF requires nine function evaluations. This modification provides a reduction in computational complexity of the estimator. Furthermore, proper selection of the parameters ξ and T presents an increase in accuracy of the estimator.

Readers are referred to the Algorithm 1 given in (Onat, 2019) for the structure of MJUKF. In addition, source codes for the application of this method to two dynamical systems have been provided by (Onat, 2020).

3. Findings and Discussion

To demonstrate the effectiveness of MJUKF against JUKF, measurements from the mechanical systems are required. Simulations based on the dynamical equations of these systems were created.

Gaussian noise was added to the simulated system states to form simulated measurements for testing JUKF and MJUKF. All simulations and estimators were coded in Python and run on an HP Z420 workstation (HP, 2024). Source codes to run and verify simulations and estimators can be found in (Onat, 2024).

To solve the differential equations of the given mechanical systems, a modified method based on the combination of the trapezoidal and the second-order backward Euler Method (abbreviated as I-TR-BDF2) is considered in this study (Onat & Örüklü, 2023). The dynamical equations for the coupled tank system and single-link flexible joint robot model have been solved using this numerical method.

After obtaining the solution for the system states, simulated measurements are created by adding Gaussian noise to the corresponding system states. The signal-to-noise ratio for both systems is 30 dB. The noisy simulated measurements are then presented in figures to demonstrate the simulation results.

First, the coupled tank system is simulated. It should be noted that the input u in Equation (2) corresponds to the pump rate q_i, which is constant and has units of Volts. This system has two states. The total simulation time for the system is 200 s, and the step size is set to 1 ms. The simulated measurements obtained by adding noise to the simulation results can be seen in Figure 4.

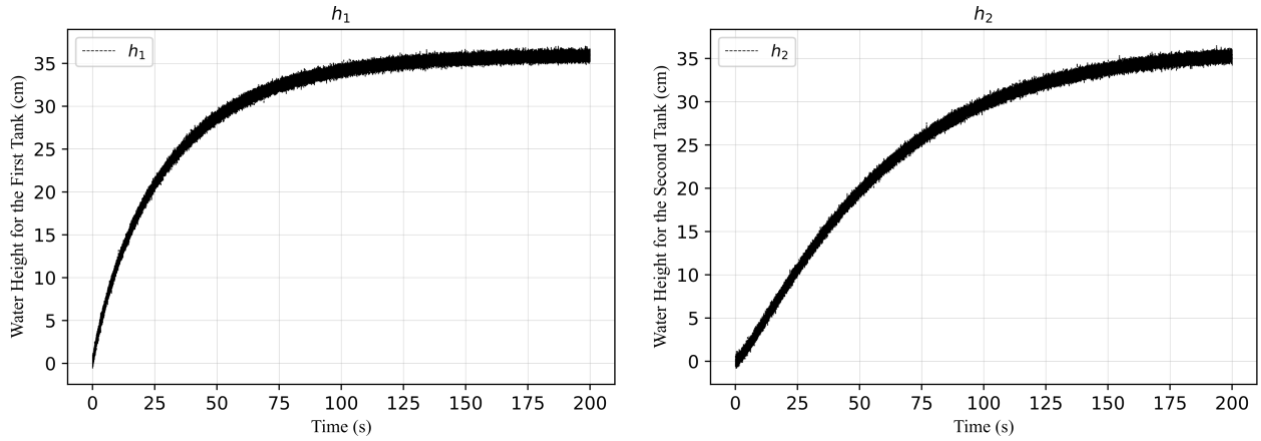

Figure 4 Simulated measurements for the coupled tank system, water levels for the first and the second tank

To simulate the single-link flexible joint robot, the input to the system has been set as $u = 5\sin(2\pi f t)$. Here, the frequency f is 1 Hz, and t is the discretized time index, denoted as kT_s in the previous section. In these simulations, the step size is set to 1 ms, and the total simulation time in this case is 20 s. The results of the simulation for the system states are presented in Figure 5 and Figure 6. Since the level of the noise (30 dB) is the same for all states, its effect is more apparent in Figure 5 than in Figure 6.

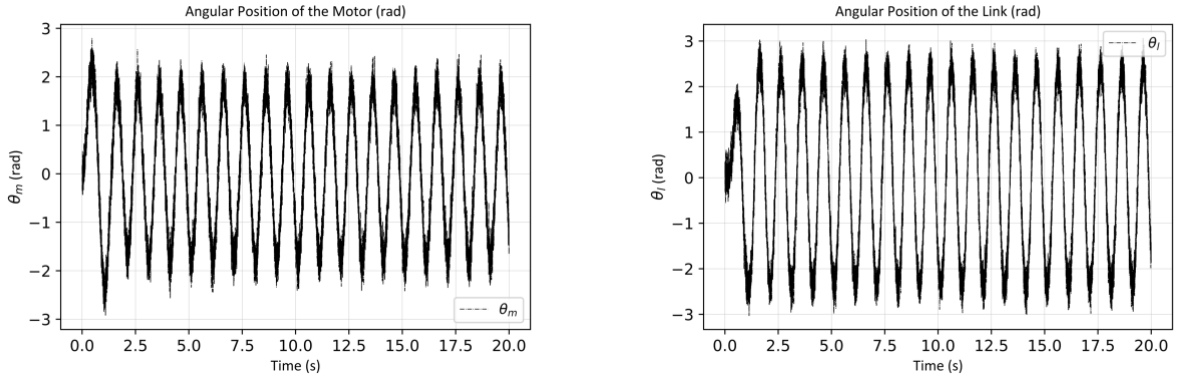

Figure 5 Simulated measurements (angular positions) for the single-link flexible joint robot

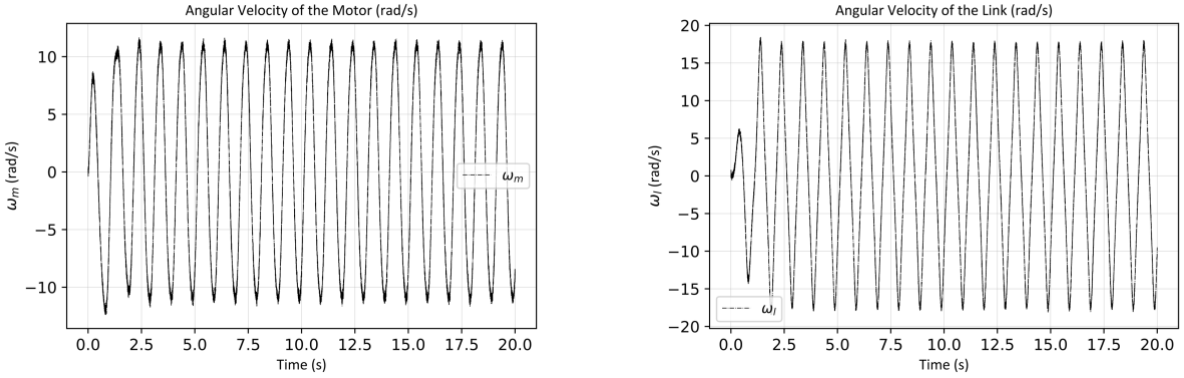

Figure 6 Simulated measurements (angular velocities) for the single-link flexible joint robot

In both cases, these results are saved and considered as the noisy measurements that can be taken from the physical system. They are used in the measurement update part of both unscented Kalman filter-based parameter estimation approaches.

The state estimation for these mechanical systems is not the focus of this modified approach. However, the state estimation results of the coupled tank system for both JUKF and MJUKF are presented in Figure 7 and Figure 8. It can be seen that both filters can effectively estimate the states of the coupled tank system. Therefore, the state estimation results for the single-link flexible joint robot model are not reported in this paper. All the initial parameters and conditions are the same for both filters. The initial state and parameter, model, and measurement noise covariance matrices are also same for both filters; initial state estimates are set to zero. Thus, a fair comparison can be made between the performance of both estimators. The initial state covariance matrix for the application of JUKF to the coupled tank system can be given as

$$\mathbf{P}_0 = \begin{bmatrix} 10^{-5} & 0 & 0 \\ 0 & 10^{-5} & 0 \\ 0 & 0 & 10^{-1} \end{bmatrix}. \tag{11}$$

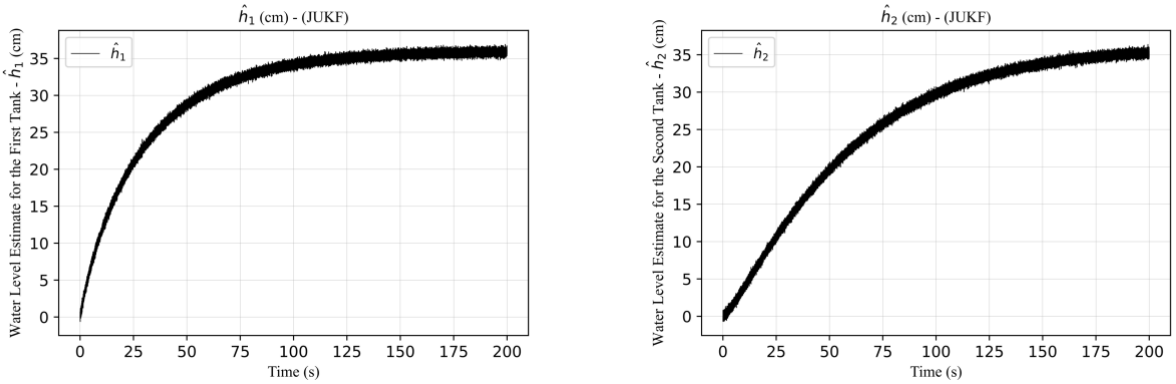

Figure 7 State estimation results for the coupled tank system based on JUKF

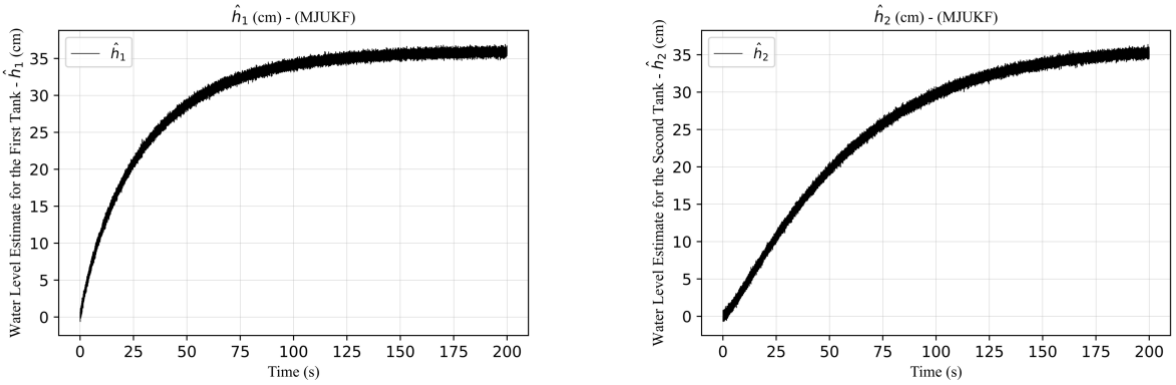

Figure 8 State estimation results for the coupled tank system based on MJUKF

It must be noticed that the first two diagonal elements are also same for the initial state covariance matrix of MJUKF. The third diagonal element of the above equation is related to the initial parameter covariance. MJUKF uses another vector (since there is one parameter to be estimated, it is a scalar) for this purpose, denoted as $\mathbf{p}_\theta$ previously. $\mathbf{p}_\theta$ is selected as $\mathbf{p}_\theta = 10^{-1}$ for MJUKF so that the level of initial parameter covariances is same for both filters. In each case, measurements from the coupled tank system are assumed to be taken once every two samples. Therefore, the sampling rate is assumed to be 2 ms (500 Hz) for both filters. The model and measurement noise covariances are given as

$$\begin{aligned} \mathbf{Q} &= \begin{bmatrix} 10^{-5} & 0 & 0 \\ 0 & 10^{-5} & 0 \\ 0 & 0 & 10^{-5} \end{bmatrix}, \\ \mathbf{R} &= \begin{bmatrix} 10^{-7} & 0 \\ 0 & 10^{-7} \end{bmatrix}. \end{aligned} \tag{12}$$

In Equation (12) $\mathbf{Q}$ is given for JUKF, and the last diagonal entry can be omitted for MJUKF. $\mathbf{R}$ is the same for both filters.

Two additional parameters related to MJUKF are needed and they are specified in Equation (9). ξ is selected as −1 and the transformation matrix (which is a vector for the coupled tank system) T is chosen as

$$T = [0.8 \quad 0.2]. \tag{13}$$

The selection of ξ and T is discussed in detail in (Onat, 2019). These parameters are chosen based on the explanations provided in (Onat, 2019). One approach for the selection of the T matrix is to evaluate the relationship between the measurements and the parameters, which can be obtained by a Jacobian matrix (Onat, 2019) and it is expressed as

$$\mathbf{J}(\theta_1, \theta_2, \dots, \theta_n) = \begin{bmatrix} \frac{\partial g_1}{\partial \theta_1} & \cdots & \frac{\partial g_1}{\partial \theta_n} \\ \vdots & \ddots & \vdots \\ \frac{\partial g_m}{\partial \theta_1} & \cdots & \frac{\partial g_m}{\partial \theta_n} \end{bmatrix}, \tag{14}$$

where m represents the number of measurement functions and n refers to the number of parameters estimated. Obviously, this approach can be considered when parameters explicitly appear in measurement equation. By interpreting the Jacobian matrix, the transformation matrix T can be expressed as

$$\begin{aligned} T &= \begin{bmatrix} t_{11} & \cdots & t_{1m} \\ \vdots & \ddots & \vdots \\ t_{n1} & \cdots & t_{nm} \end{bmatrix}, \\ \sum_{j=1}^{m} t_{ij} &= 1. \quad i = 1, \dots, n \end{aligned} \tag{15}$$

The last equation simply indicates that the effect of parameter changes on measurements must be taken into account. If a parameter has a more significant impact on a measurement than the other parameters, the corresponding value for that parameter in transformation matrix T must be selected higher than the values for other parameters. From Equation (13), it can be concluded that the influence of the first measurement on parameter estimation is greater than that of the second measurement.

Parameter estimation (coupled tank system) results for both JUKF and MJUKF can be found in Figure 9. The initial parameter estimate k_{flow} is 2 for both estimators. The root mean squared error (RMSE) of the parameter estimates with respect to the real parameter value is considered as the evaluation and comparison metric and it is expressed as

$$\sqrt{\frac{\sum_{i=1}^{N}\left(\theta-\hat{\theta}_i\right)^2}{N}}, \tag{16}$$

where θ is the actual value and N is the number of samples.

The results for the parameter estimation of the coupled tank system are given in Table 3. It can be seen from the results that MJUKF provides a parameter estimate with less RMSE compared to JUKF. While improving the accuracy in terms of RMSE, MJUKF also enhances the computational complexity. To evaluate computation time, each method is run twenty times, and the average elapsed time is given in Table 3.

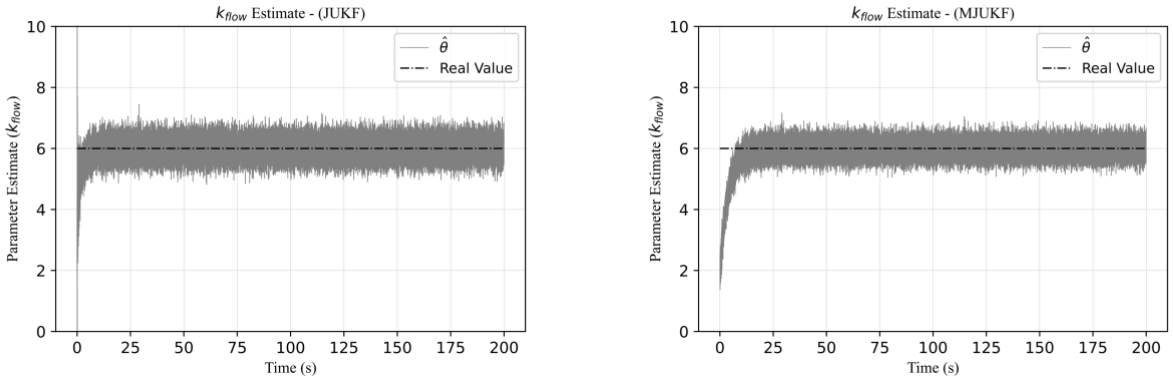

Figure 9 Parameter estimation results for the coupled tank system (JUKF result on the left figure and MJUKF result on the right figure)

Table 3 Comparison of the parameter estimate (k_{flow}) of the estimators for coupled tank system.

Metric	JUKF	MJUKF
RMSE	0.2919	0.2434
Computation Time (s)	77.696	71.191

The state estimation results for the single-link flexible joint robot are not presented here for clarity. In this case, it can be seen from the given state space equations (Equation (4)) that there are a total of four states. It has been assumed that all states of the system are measurable. The parameter estimation is carried out for two parameters of the single-link flexible joint robot: the amplifier gain K_τ and the pointer mass m. The initial state covariance matrix for the application of JUKF to the single-link flexible joint robot can be given as

$$\mathbf{P}_0 = \begin{bmatrix} 0.5 & 0 & 0 & 0 & 0 & 0 \\ 0 & 0.5 & 0 & 0 & 0 & 0 \\ 0 & 0 & 0.5 & 0 & 0 & 0 \\ 0 & 0 & 0 & 0.5 & 0 & 0 \\ 0 & 0 & 0 & 0 & 0.001 & 0 \\ 0 & 0 & 0 & 0 & 0 & 0.001 \end{bmatrix}. \tag{17}$$

It should be noted that this system includes four states and two parameters to be estimated. Therefore, the last two diagonal elements of the initial state covariance matrix are for the parameter estimates. MJUKF uses another vector for $\mathbf{p}_\theta$ the parameter estimation. It is selected as $\mathbf{p}_\theta = [0.01 \quad 0.01]$. As in the first application, all conditions are the same for both JUKF and MJUKF. The model and measurement noise covariance matrices are given as

$$\mathbf{Q} = \begin{bmatrix} 10^{-5} & 0 & 0 & 0 & 0 & 0 \\ 0 & 10^{-5} & 0 & 0 & 0 & 0 \\ 0 & 0 & 10^{-5} & 0 & 0 & 0 \\ 0 & 0 & 0 & 10^{-5} & 0 & 0 \\ 0 & 0 & 0 & 0 & 10^{-5} & 0 \\ 0 & 0 & 0 & 0 & 0 & 10^{-5} \end{bmatrix},$$
$$\mathbf{R} = \begin{bmatrix} 10^{-3} & 0 & 0 & 0 \\ 0 & 10^{-3} & 0 & 0 \\ 0 & 0 & 10^{-3} & 0 \\ 0 & 0 & 0 & 10^{-3} \end{bmatrix}. \tag{18}$$

The equation above includes **Q** for JUKF. Since there are two parameters to be estimated, the last two rows and columns can be omitted from **Q** for the application of MJUKF. **R** is the same for both filters.

For MJUKF, the parameter ξ is selected as $\xi = -0.0025$, and the transformation matrix T is chosen as

$$T = \begin{bmatrix} 0.3 & 0.3 & 0.2 & 0.2 \\ 0.2 & 0.2 & 0.3 & 0.3 \end{bmatrix}. \tag{19}$$

Parameter estimation results for this case are given in Figure 10 and Figure 11. In each case, measurements are assumed to be taken once every five samples. Therefore, the sampling rate is 5 ms (200 Hz) for both filters. The step size for the solution is also the same for this system, and it is 1 ms.

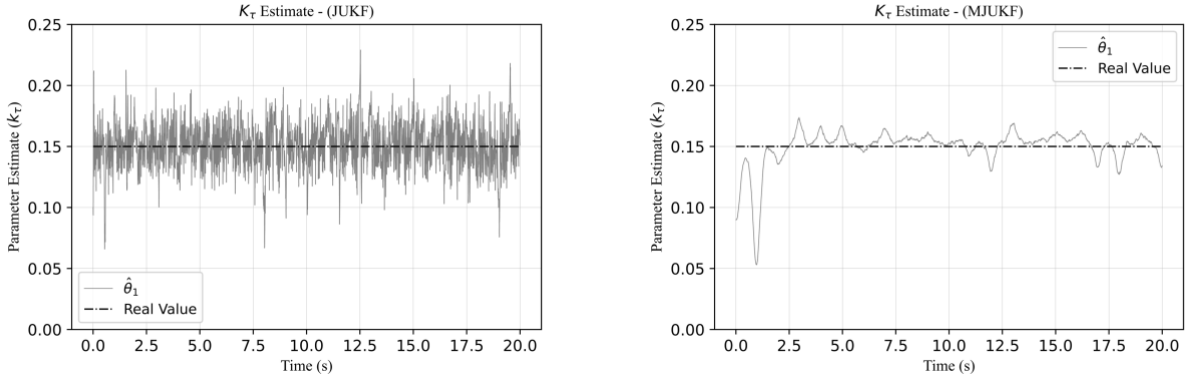

Figure 10 Parameter (K_τ) estimation results for the single-link flexible joint robot

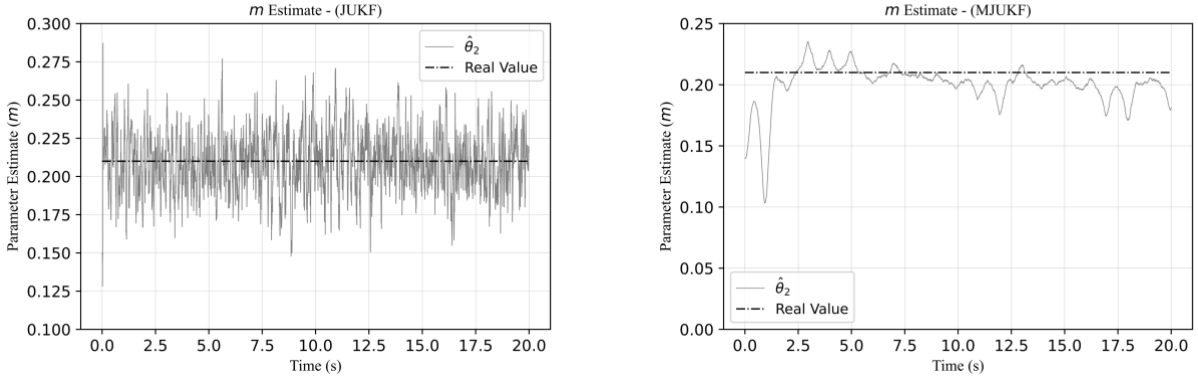

Figure 11 Parameter (m) estimation results for the single-link flexible joint robot

It is evident from Table 4 that MJUKF significantly improves the parameter estimation results in terms of RMSE and computation time. Computation time decreases more than the first application case (coupled tank system) since the number of parameters to be estimated is higher than the first application. The trends for parameter estimation of the coupled tank system with both JUKF and MJUKF are the same, as shown in Figure 9. However, in the second case, the trend for MJUKF is smoother than for JUKF. The main reason is the selection of the scaling parameter ξ along with the transformation matrix T. For the coupled tank system, the scaling parameter is selected as unity, whereas, for the single-link flexible joint robot, it is a small value $\xi = -0.0025$. This selection provides a smoothing effect in the application of MJUKF to the single-link flexible joint robot.

Table 4 Comparison of the parameter estimates (K_τ and m) of the estimators for single–link flexible joint robot.

Metric	JUKF	MJUKF
RMSE (K_τ)	0.0177	0.008
RMSE (m)	0.019	0.01233
Computation Time (s)	4.337	3.717

To demonstrate the performance of the MJUKF in cases of parameter changes, an additional simulation study has been defined. In this case, it is assumed that at $t = 5$ seconds, the system

parameters of the single-link flexible joint robot change. After five seconds, the mass changes from $m = 2.1 \times 10^{-1}$ to $m = 3 \times 10^{-1}$, and the amplifier gain changes from $K_\tau = 15 \times 10^{-2}$ to $K_\tau = 10 \times 10^{-2}$. It is evident from Figure 12 and Figure 13 that the parameter estimates of the JUKF and MJUKF can both track the parameter changes of the physical system.

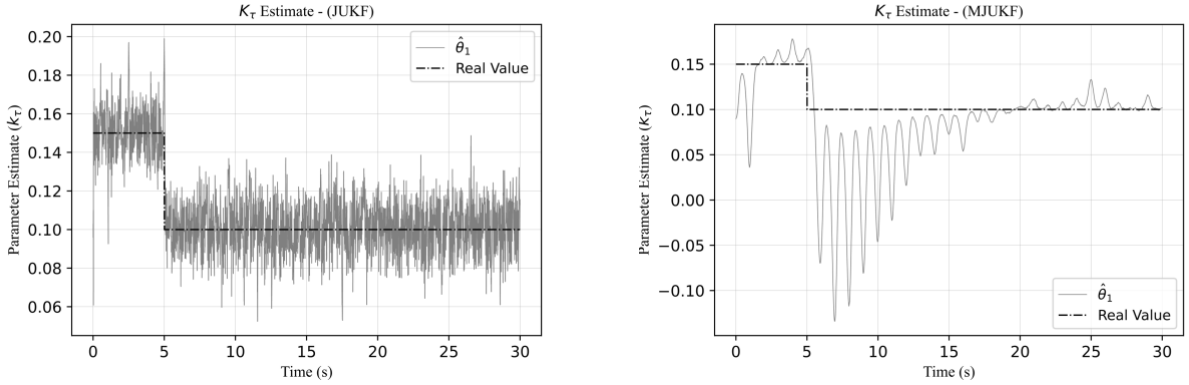

Figure 12 Parameter (K_τ) estimation results for the single-link flexible joint robot, at time $t = 5$ seconds parameter value changes

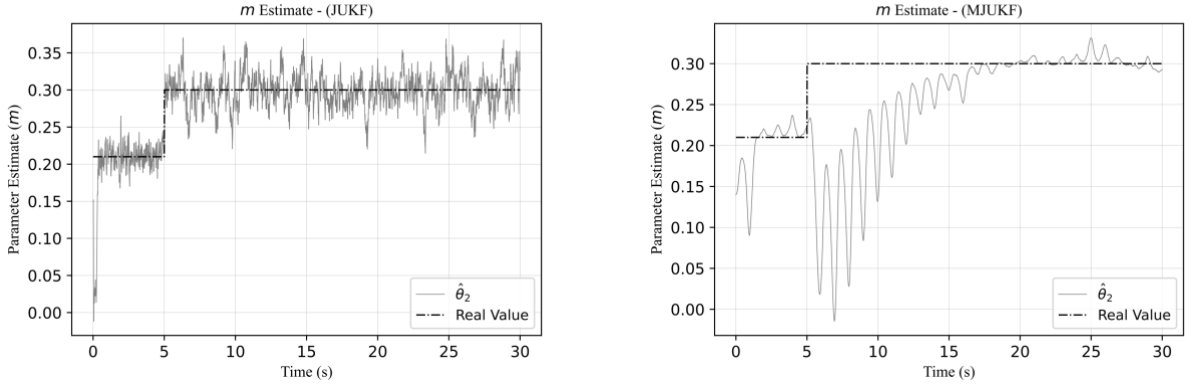

Figure 13 Parameter (m) estimation results for the single-link flexible joint robot, at time $t = 5$ seconds parameter value changes

The convergence of the MJUKF in this case is evidently slow due to the choice of the scaling parameter ξ. As a result, the estimation duration is extended to 30 seconds for both JUKF and MJUKF.

It should again be noted that the scaling parameter ξ is critical for parameter estimation by MJUKF. A value of ξ that is too large may lead to system instability and accuracy issues, while a value that is too small may slow convergence. Therefore, estimation performance strongly depends on this parameter (Onat, 2019). In cases of parameter change, ξ can be set to -0.0035 for the MJUKF to achieve faster convergence. Although $\xi = -0.0025$, as used in the previous simulation study, it also leads to convergence, $\xi = -0.0035$ is chosen here to both demonstrate the adaptability of MJUKF to parameter changes and illustrate its performance with a properly selected filter parameter.

As shown in Figure 14, MJUKF responds to parameter changes more quickly, and accurately under steady-state conditions. Future work for the MJUKF includes the development of an adaptive scaling parameter.

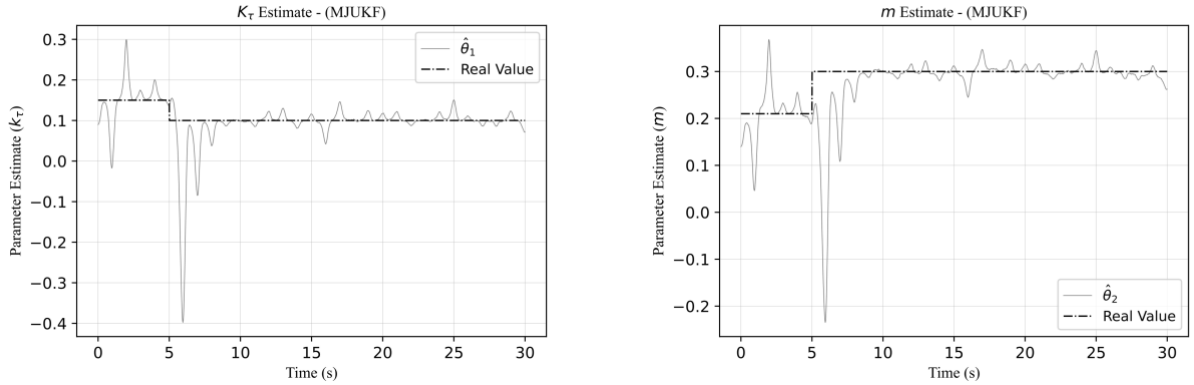

Figure 14 Parameter estimation results for the single-link flexible joint robot with MJUKF, at time $t = 5$ seconds parameter value changes and the scaling parameter is $\xi = -0.0035$

In short, the results demonstrate that MJUKF is a promising alternative to standard JUKF for parameter estimation of a class of nonlinear mechanical systems when there is a linear relationship with the measurements and the estimated parameters.

4. Conclusions and Recommendations

In this study, a modified joint unscented Kalman filter-based parameter estimator is applied to two selected mechanical systems. This method has been previously applied to other dynamical systems in (Onat, 2019). To the author's knowledge, this is the first study in which this modified scheme is applied for the parameter estimation of such mechanical systems.

It should be noted that the modified approach used here can be applied to systems where there is a linear relationship between the measurements and the parameters. The results reveal that the MJUKF can estimate the parameters of such mechanical systems more accurately than the JUKF. Not only the MJUKF improves accuracy, but it also decreases computational complexity. These results are presented in Table 3 and Table 4.

Acknowledgements

The author thanks his student, Batuhan Mert Düzen, for preparing the figures of the considered mechanical systems. The author would also like to thank Kerim Örüklü for proofreading the text.

The author used ChatGPT (GPT-3, OpenAI's large-scale language-generation model) to correct typographical, grammatical, and other types of errors in this text. The author reviewed, edited, and revised the corrections made by ChatGPT and takes ultimate responsibility for the content of this publication.

Authors' Contributions

The author was solely responsible for all aspects of this research, including conceptualization, methodology, data collection, data analysis, and manuscript writing.

Statement of Conflicts of Interest

The author declares that there are no conflicts of interest associated with this work.

Statement of Research and Publication Ethics

The author declares that this study complies with Research and Publication Ethics.

References

González-Cagigal, M. A., Rosendo-Macías, J. A., & Gómez-Expósito, A. (2019). Parameter estimation of fully regulated synchronous generators using unscented Kalman filters. Electric power systems research, 168, 210–217.

González-Cagigal, M. Á., Rosendo-Macías, J. A., & Gómez-Expósito, A. (2022). State and Parameter Estimation of Photovoltaic Modules using Unscented Kalman Filters. RE&PQJ, 20.

Gonzólez-Cagigal, M. Á., Rosendo-Macías, J. A., & Gómez-Expósito, A. (2022). Parameter estimation for hot-spot thermal model of power transformers using unscented Kalman filters. Journal of Modern Power Systems and Clean Energy, 11, 634–642.

HP. (2024, April 01). HP Z420 Workstation Product Specifications. Retrieved from https://support.hp.com/us-en/document/c03277050

Onat, A. (2019). A novel and computationally efficient joint unscented Kalman filtering scheme for parameter estimation of a class of nonlinear systems. Ieee Access, 7, 31634–31655.

Onat, A. (2020). Source Code: A Novel and Computationally Efficient Joint Unscented Kalman Filtering Scheme for Parameter Estimation of a Class of Nonlinear Systems. Retrieved from https://github.com/altanonat/MJUKF

Onat, A. (2024). Source Code: Application of a Modified Joint Unscented Kalman Filter for Parameter Estimation of a Class of Mechanical Systems. Retrieved from Github: https://github.com/altanonat/mjukf-application

Onat, A., & Kayaalp, B. T. (2020). A joint unscented Kalman filter-based dynamic weigh in motion system for railway vehicles with traction. IEEE Sensors Journal, 21, 15709–15718.

Onat, A., & Örüklü, K. (2023). A New Numerical Approach for Simulation of Power Electronics Converters. 14th International Conference on electrical and Electronics Engineering (ELECO) (pp. 1-5). IEEE.

Onat, A., Voltr, P., & Lata, M. (2018). An unscented Kalman filter-based rolling radius estimation methodology for railway vehicles with traction. Proceedings of the Institution of Mechanical Engineers, Part F: Journal of Rail and Rapid Transit, 232, 1686–1702.

Pei, X., Chen, Z., Yang, B., & Chu, D. (2020). Estimation of states and parameters of multi-axle distributed electric vehicle based on dual unscented Kalman filter. Science progress, 103, 0036850419880083.

Peng, N., Zhang, S., Guo, X., & Zhang, X. (2021). Online parameters identification and state of charge estimation for lithium-ion batteries using improved adaptive dual unscented Kalman filter. International Journal of Energy Research, 45, 975–990.

Raghavan, S., & Hedrick, J. K. (1994). Observer design for a class of nonlinear systems. International Journal of Control, 59, 515–528.

Seung, J.-H., Atiya, A. F., Parlos, A. G., & Chong, K.-T. (2017). Identification of unknown parameter value for precise flow control of Coupled Tank using Robust Unscented Kalman filter. International Journal of Precision Engineering and Manufacturing, 18, 31–38.

Uysal, C., Onat, A., & Filik, T. (2020). Non-contact respiratory rate estimation in real-time with modified joint unscented Kalman filter. Ieee Access, 8, 99445–99457.

Van Der Merwe, R. (2004). Sigma-point Kalman filters for probabilistic inference in dynamic state-space models. Oregon Health & Science University.